

Laboratory for Energy and NanoScience

COMPENDIUM

CHAPTER 2:

Reconstructing force profiles with an
amplitude-modulation AFM in tapping
mode

**LENS COMPENDIUM**Published July 2020

Authors:Tuza Olukan¹Chia Yun Lai¹Sergio Santos^{1,3}Carlo Alberto Amadei⁴Matteo Chiesa^{1,2}**Corresponding author:** Tuza Olukan - Tuzaolukan@gmail.com**Affiliations:**

1. Department of Physics and Technology, UiT The Arctic University of Norway, Tromsø, Norway
2. Laboratory for Energy and NanoScience (LENS), Khalifa University of Science and Technology, Masdar Campus, Abu Dhabi, UAE
3. Future Synthesis, Skien, Norway
4. The World Bank, 1818 H Street, NW Washington, DC 20433 USA

Design and layout: Maritsa Kissamitaki¹

CONTENTS

Reconstructing force profiles with an amplitude-modulation AFM in tapping mode.....	3
Steps to collect the raw data to reconstruct force profiles	5
Steps to process the raw data	7
Examples of force reconstruction	9
Brief summary of the theory of conservative forces in AFM.....	11
Bibliography	14

Reconstructing force profiles with an amplitude-modulation AFM in tapping mode

Here we demonstrate how to reconstruct force profiles with an amplitude-modulation AFM operated in standard tapping mode. Our example is based on the Cypher scanning probe microscope from Asylum Research. The method is based on Sader and Katan's algorithm, but we have implemented an experimental set-up that allows for robust reconstruction. We discuss the details here.

Brief introduction of the force reconstruction method

The use of AFM has also been exploited in force spectroscopy wherein one reconstructs the nanoscale force profile from experimental observables to recover the force as a function of tip-sample separation distance (d)¹⁻²⁶ (Figure 1).

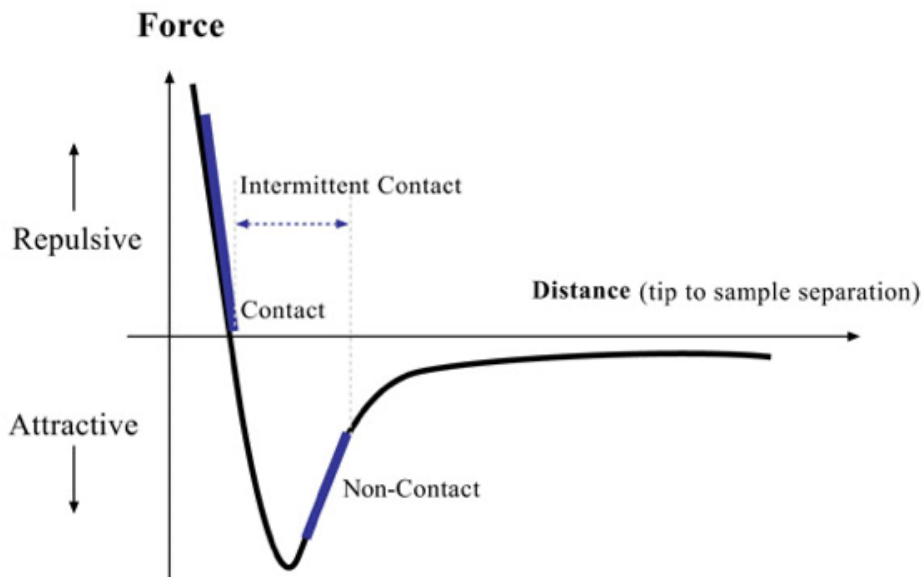


Figure 1: Force vs Distance curve.

In dynamic AFM, the integral form of the equation of motion can be reduced to a standard driven harmonic oscillator with damping and the addition of the tip-sample force that introduces the non-linearities. Here, the method used to reconstruct the force-distance curves (FDCs) is the Sader-Jarvis-Katan formalism^{20,27,28}, which is a derivation of the results obtained via the Laplace transform. The FDCs are reconstructed by considering variations in cantilever amplitude (A) and phase (P) as a function of variations in separation distance d . Noted that the free amplitude of tip oscillation A_0 is a key parameter to achieve a smooth transition to the repulsive regime, *i.e.*, avoiding bistability and discontinuity in the amplitude-phase-distance curves^{29,30}. Usually, A_0 is set to 3 times higher than the critical amplitude A_c value³¹⁻³³, which is the minimum free amplitude A_0 required to reach the repulsive regime.

Steps to collect the raw data to reconstruct force profiles

1. First, approach the tip as discussed in the previous article.

2. Perform a force-distance curve once while setting the force distance to 30 - 50 nm (Figure 2).

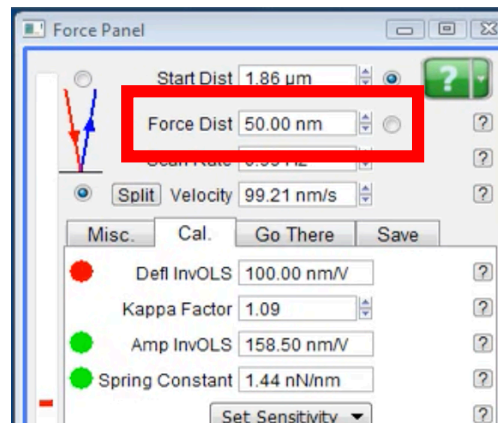


Figure 2

3. Perform the Thermal test again. After the thermal test, copy the frequency on the thermal tab and paste it in the main tab of the master panel (Figure 3).

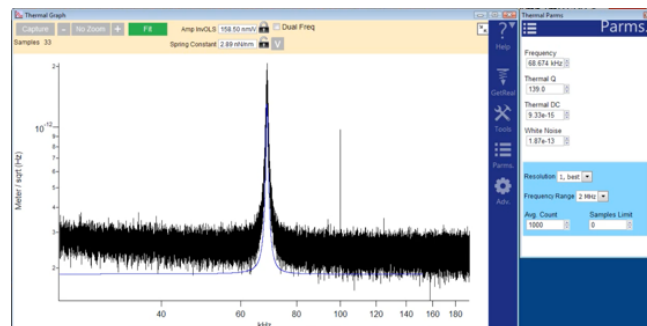


Figure 3

4. Next, find the A_c as discussed in the previous article.

5. Run a force-distance curve again while setting the force distance to 150-200 nm (Figure 4).

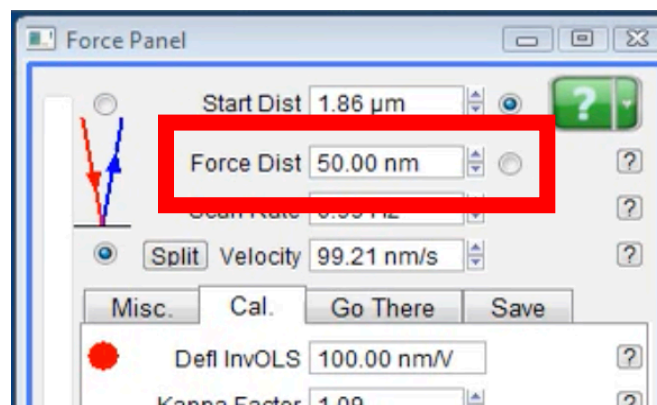


Figure 4

- Set the free amplitude to 3-5 times of the critical amplitude value, and the trigger point to 95% of the free amplitude value (Figure 5).

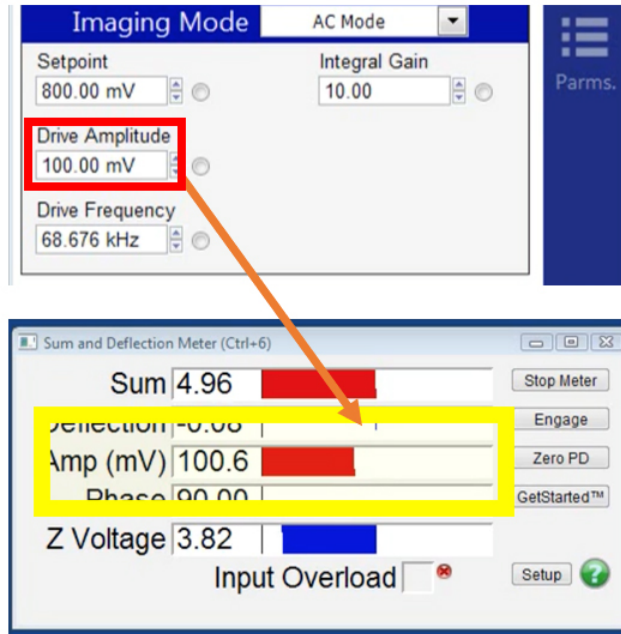


Figure 5: Amplitude (yellow) can be adjusted from the drive's amplitude button (red). The value can also be tuned from the wheel knob.

- Adjust the force distance to 10-25 nm depending on the tip-sample interaction (Figure 6).

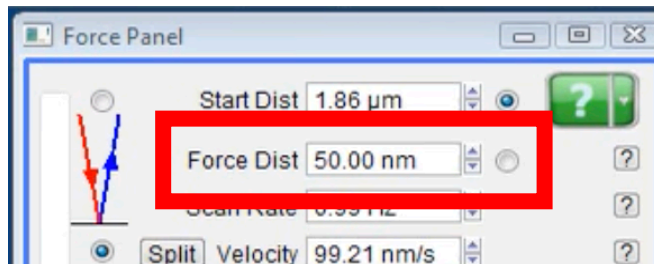


Figure 6

8. Adjust the trigger point according to the phase channel. Allow the phase lag to reach $\sim 80^\circ$ (Figure 7).

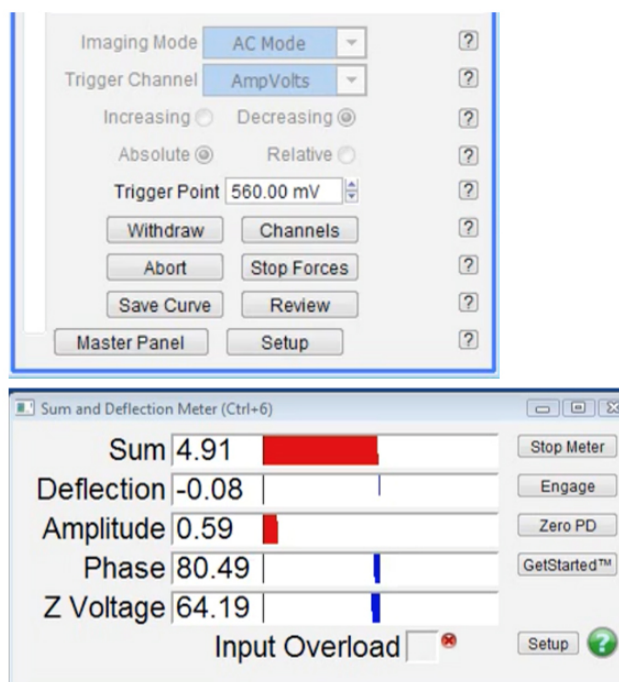


Figure 7

9. After all the parameters are set, click “Continuous” to collect the data (Figure 8).

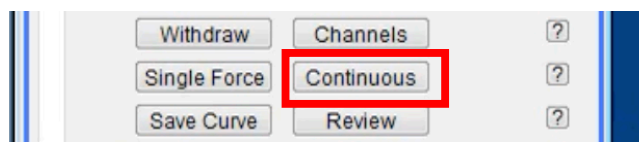


Figure 8

Steps to process the raw data

Note: R studio needs to be installed and add to the path. All the source codes can be found [here](#).

- Copy the IBW files into the `UNPACKIGOR\FILES` folder and run the Matlab file: `UnpackAND_ShuffleName_IgorFiles` (Figure 9).

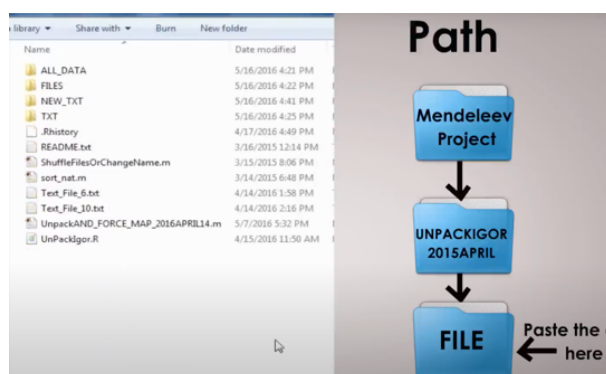


Figure 9

- NEW_TXT* folder will be generated when the code finishes running and renames the folder if needed (Figure 10).

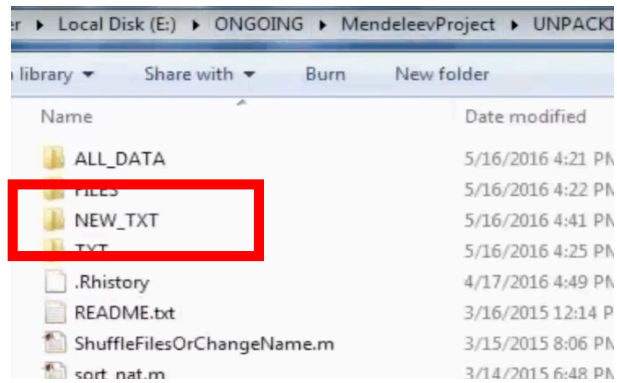


Figure 10: Copy the new test from this directory.

- Copy the *NEW_TXT* (or rename) folder into *FORCE_AMAFM_2015APRIL\DATA_SET* folder and run the Matlab file: *Forces_Paralel_2015March24* (Figure 11).

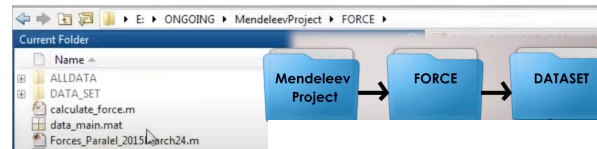


Figure 11

- Spring constant, Q factor, and Amplitude inVolts can be changed according to the calibration results (Figure 12).

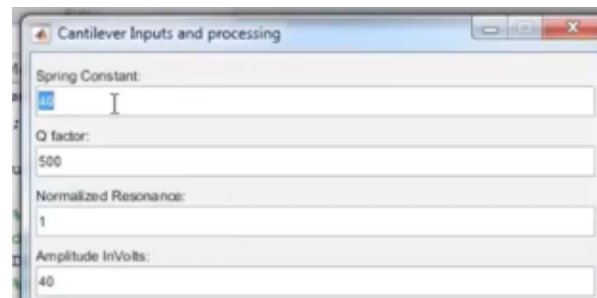


Figure 12

- PROCESSED_SETS.mat* file will be generated when the code finishes running and renames the file if needed (Figure 13).

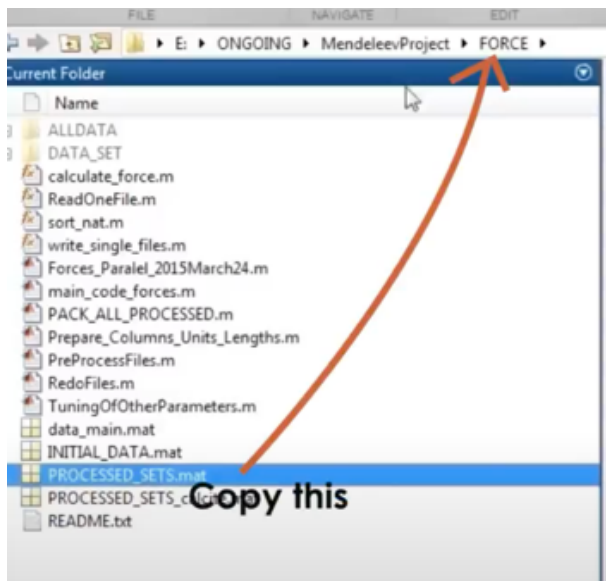


Figure 13

- Copy the PROCESSED_SETS.mat or the renamed file into STATS2015APRIL24 folder and run the Matlab file: MainStatistics2015MAY12 (Figure 14).

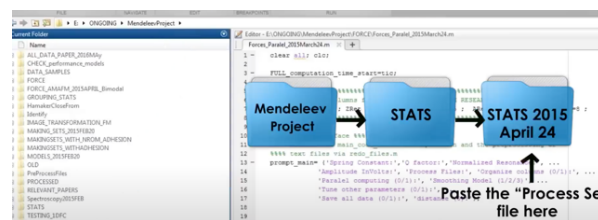


Figure 14

- ALL_DATA_STATS.mat will be generated when the code finishes running and renames the file if needed (Figure 15).

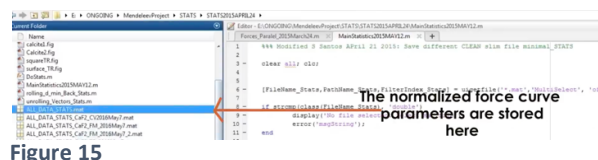


Figure 15

Examples of force reconstruction

The procedure just discussed leads us to an experimentally reconstructed tip-surface force profile that is an average of several experimental amplitude versus phase distance curves. An example is shown in Figure 16 as reproduced from Ref. 18. In this work we were looking at carbonate formation layers on calcite. The histograms show two phases on the surface, one where the carbonate layers have formed and the other where it has not. This provides us with a marker to study the formation.

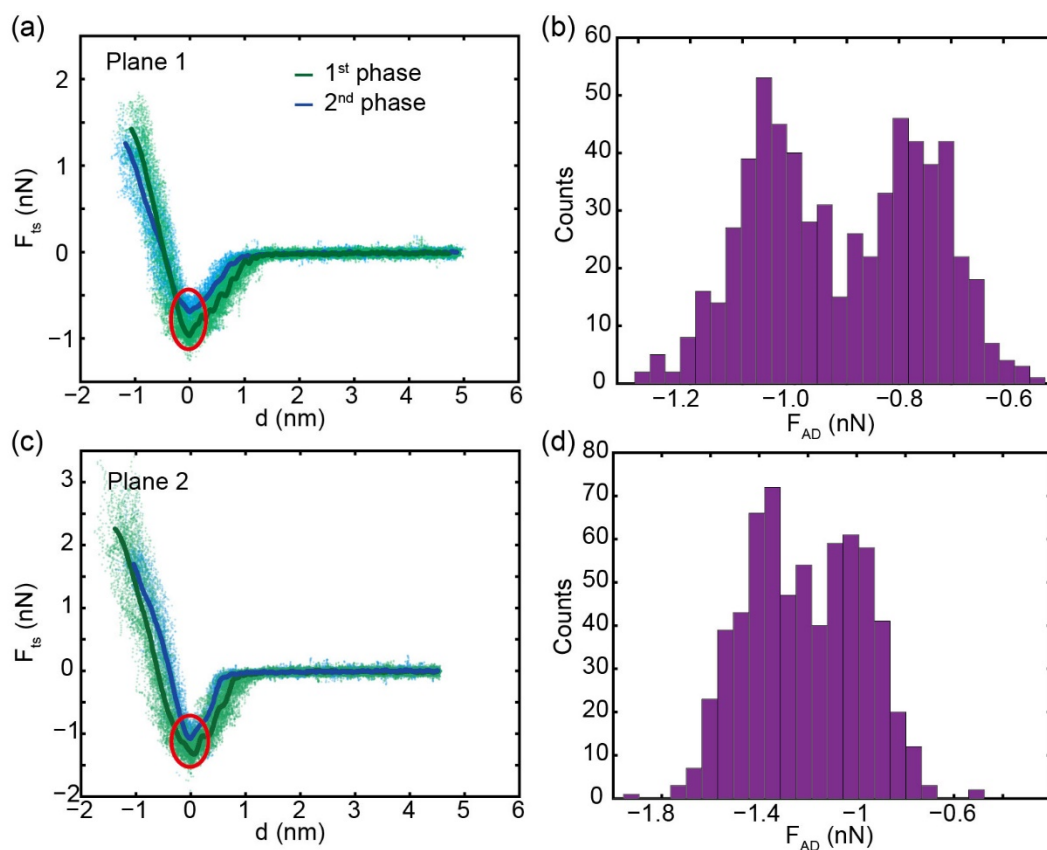


Figure 16. Force profiles for both phases on plane 1. (b) Histogram of F_{AD} for the 1st and 2nd phase one plane 1. (c) Reconstructed force curves on plane 2. (d) F_{AD} histogram for both phases on plane 2. Blue and green dots represent for experimental data while the continuous lines stand for averaged force curves.

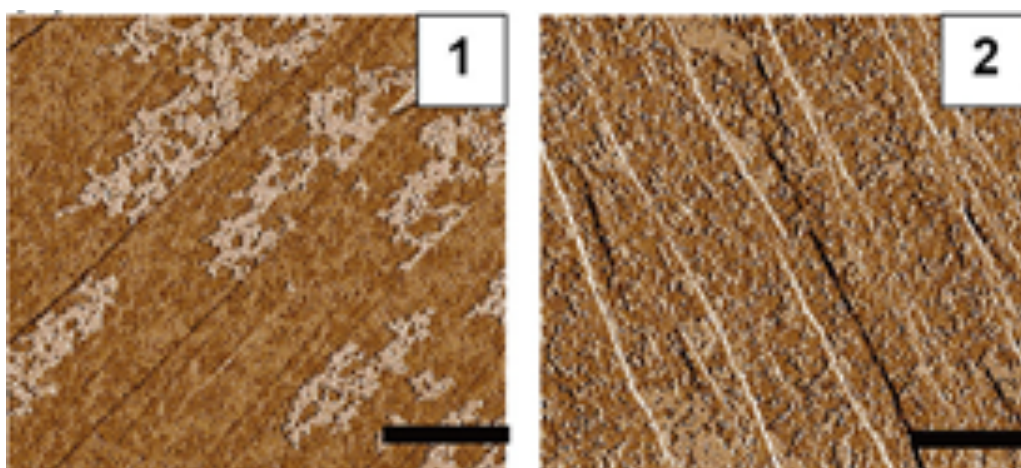


Figure 17. AFM phase images for 2 calcite cleavage planes. Scale bar: 500 nm corresponding to the forces in Figure 16. (Ref. 18)

Brief summary of the theory of conservative forces in AFM

In the paper “Spatial horizons in amplitude and frequency modulation atomic force microscopy”³⁴, and many several others, we discuss long range and short range conservative forces. These forces vary as a function of tip-surface distance and cover an area of interaction. This means that these forces do not affect an infinitesimal point in space. This is shown in Figure 18 as reproduced from the paper.

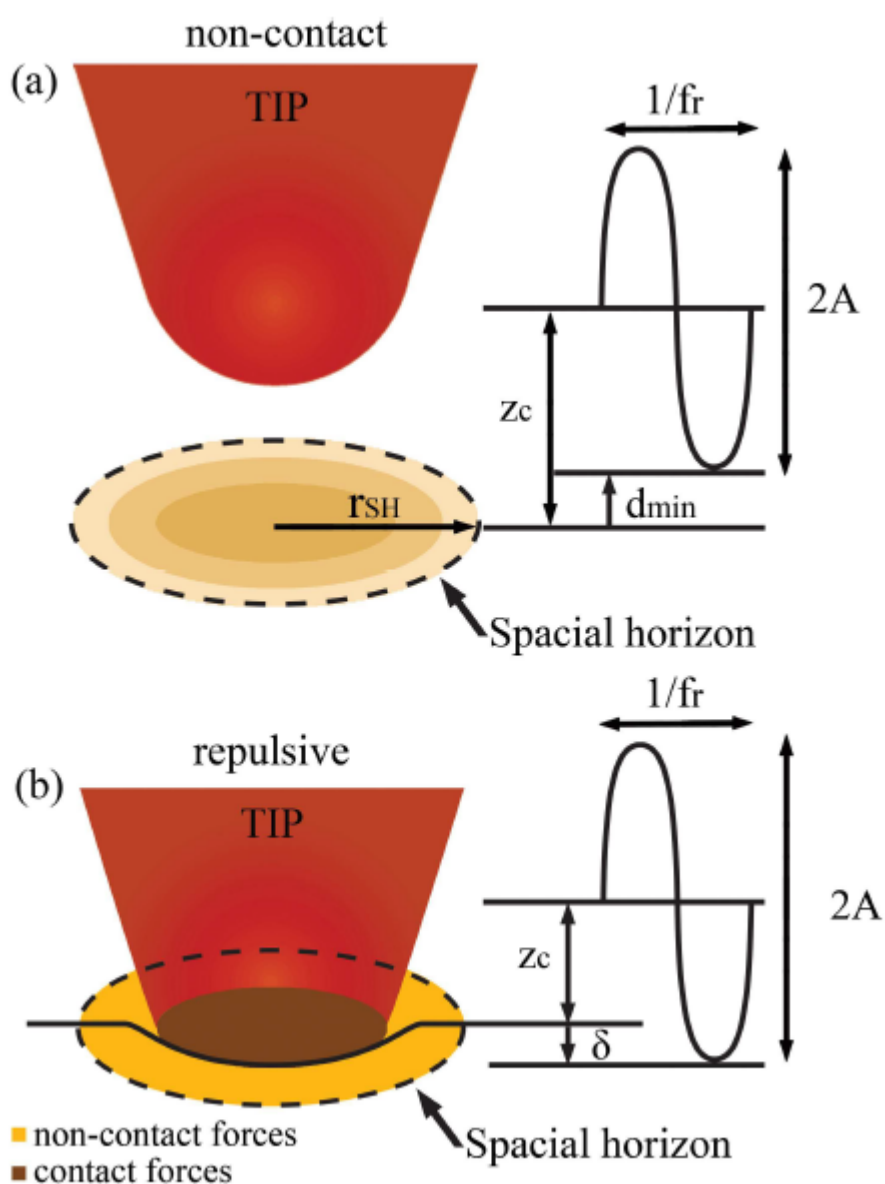


Figure 18. (a) Scheme of a tip vibrating in the non-contact mode where $d_{min} > a_0$ and $\delta = 0$. The Spatial Horizon (SH) is thus affected by long range forces only. The interactions

occurring between the tip and the sample's atoms lying beyond the boundary established by the SH do not sufficiently affect the dynamics of the cantilever for the feedback to detect them. (b) Scheme of a tip vibrating in the repulsive regime where intermittent mechanical contact occurs $d_{\text{min}} > a_0$ and $\delta > 0$. The SH in this case is affected by both short range and long range forces.

Molecularly or atomically, these forces can be understood as atomic interactions between atoms as described in Ref. 21.

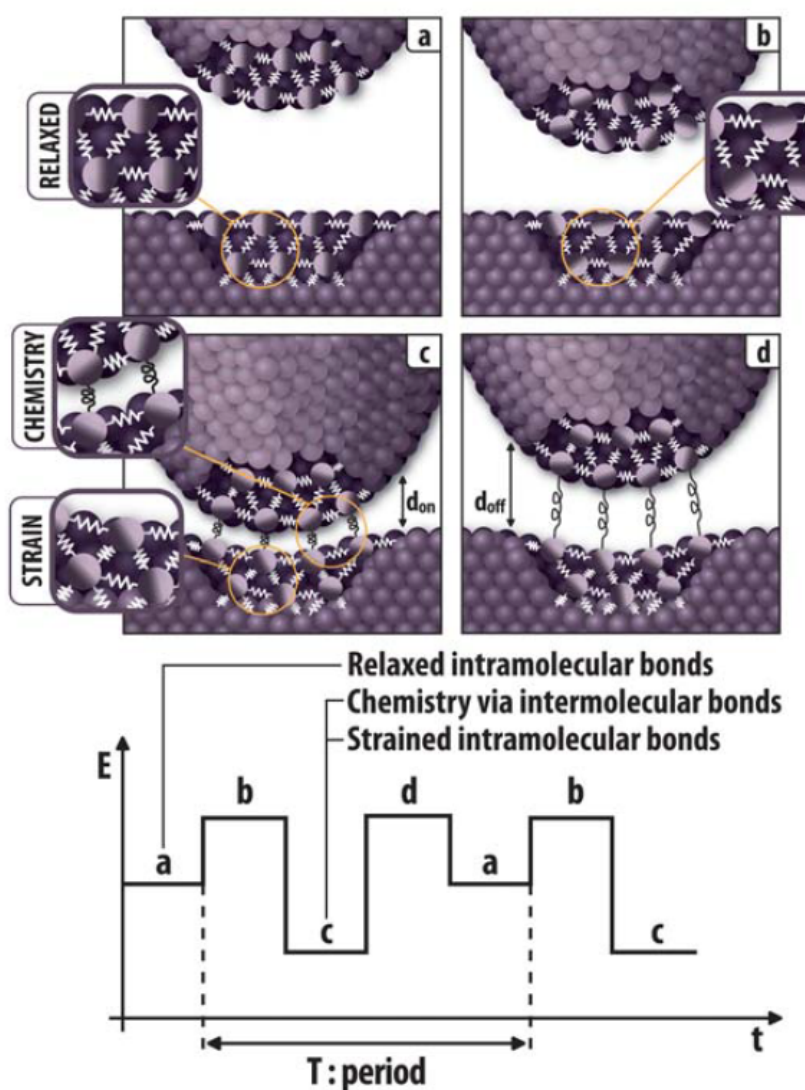


Figure 19. a-d) Illustrations representing electron and spatial configuration of atoms in a tip and a sample. The scheme describes the phenomena that might be involved during

induced mutual tip-sample intermolecular and intermolecular interactions as the tip approaches and retracts from the sample. A scheme illustrating the evolution of the interaction energy E during a full oscillation period is shown at the bottom. In the same article we discuss the way in which the raw curves in AM AFM, that is, the phase and amplitude, vary with the different forces. In the article we discuss both dissipative and conservative forces.

We would also like to inform the reader that in the presence of water on surfaces, in ambient AFM, several other forces should be considered. An illustration of this phenomenon is shown in Figure 20 as reproduced from “Capillary and van der Waals interactions on CaF₂ crystals from amplitude modulation AFM force reconstruction profiles under ambient conditions”³⁵. You can see how nanometric water layers form both on the tip and the sample and this can have effects on topography as shown in the figure.

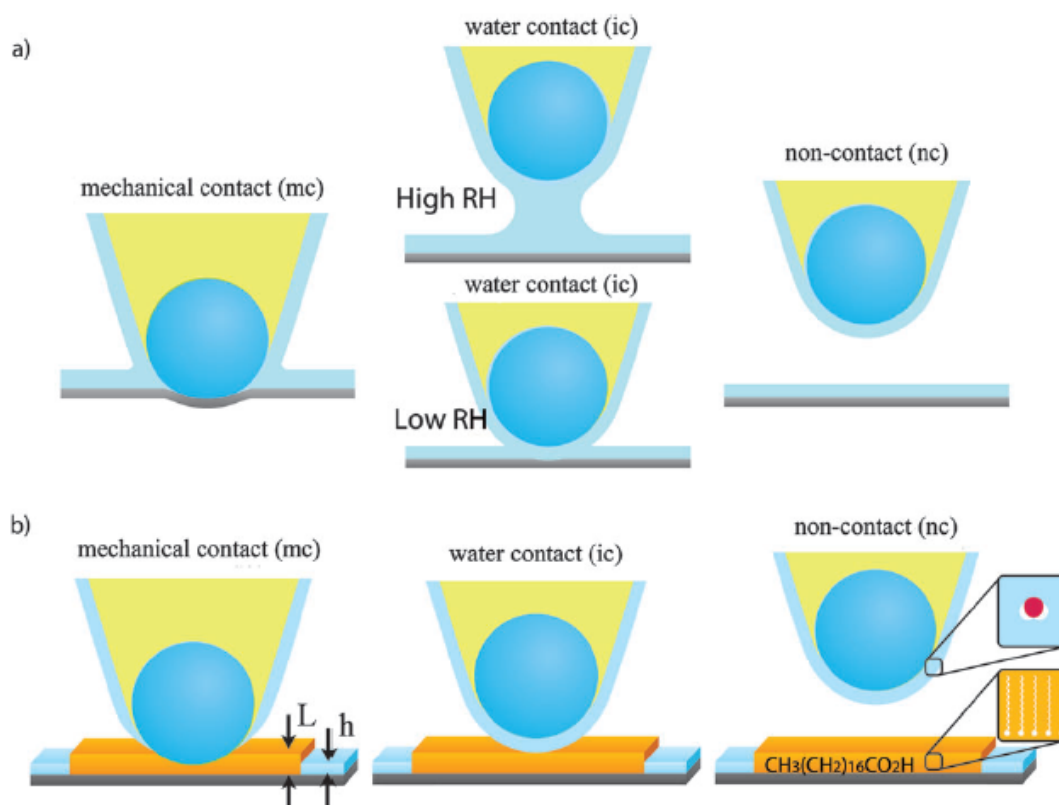


Figure 20. Schemes showing the different interaction regimes, non-contact (nc), intermittent contact (ic) and mechanical contact (mc) on (a) a hydrophilic surface (i.e., mica) and (b) hydrophobic stearic SAM (top) and hydrophilic mica (bottom) as it has been considered in the simulations. Water layers are considered to exist only on the mica and the tip surface. Water neck formation (capillary) is only considered on the mica surface when under high RH conditions.

The sharpness of the tip also affects the forces as shown in the illustration in Figure 21 as reproduced from the paper “Size Dependent Transitions in Nanoscale Dissipation”³⁶.

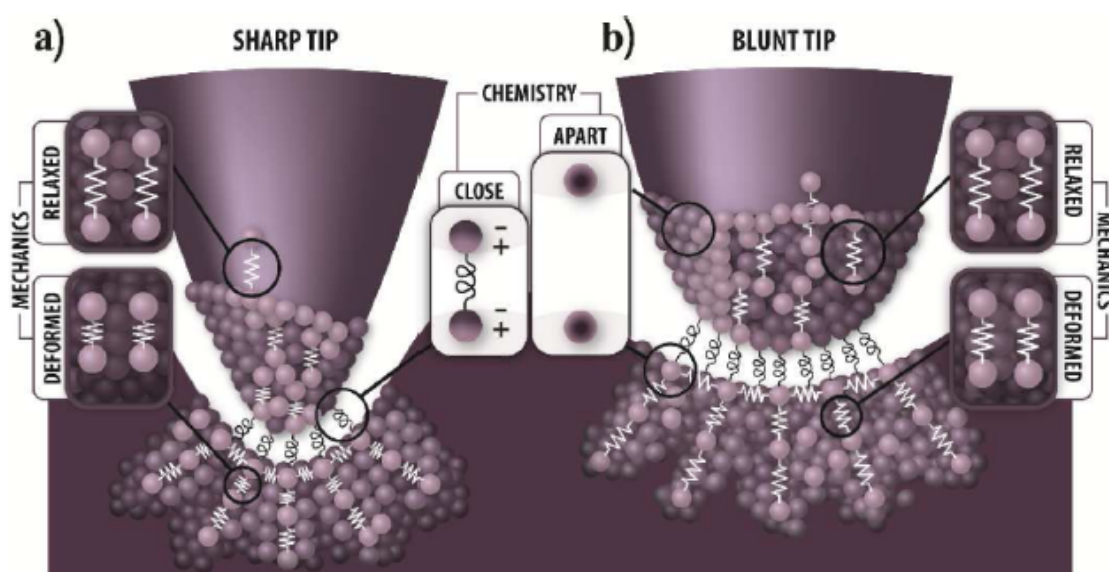


Figure 21. Scheme of the possible interactions occurring between an AFM tip and a surface when (a) the tip is very sharp and (b) when it becomes blunter.

Bibliography

- 1 Santos, S. *et al.* Stability, resolution, and ultra-low wear amplitude modulation atomic force microscopy of DNA: Small amplitude small set-point imaging. *Appl. Phys. Lett.* **103**, 063702, doi:doi:<http://dx.doi.org/10.1063/1.4817906> (2013).
- 2 Lai, C.-Y. *et al.* A nanoscopic approach to studying evolution in graphene wettability. *Carbon* **80**, 784-792, doi:<http://dx.doi.org/10.1016/j.carbon.2014.09.034> (2014).
- 3 Amir, F. P., Daniel, M.-J. & Ricardo, G. Force reconstruction from tapping mode force microscopy experiments. *Nanotechnology* **26**, 185706 (2015).
- 4 Tamalampudi, S. R. *et al.* Rapid discrimination of chemically distinctive surface terminations in 2D material based heterostructures by direct van der Waals identification. *Review of Scientific Instruments* **91**, 023907, doi:10.1063/1.5128756 (2020).
- 5 Lai, C.-Y. *et al.* Explaining doping in material research (Hf substitution in ZnO films) by directly quantifying the van der Waals force. *Physical Chemistry Chemical Physics* **22**, 4130-4137, doi:10.1039/C9CP06441A (2020).
- 6 Lai, C.-Y., Santos, S. & Chiesa, M. Machine learning assisted quantification of graphitic surfaces exposure to defined environments. *Appl. Phys. Lett.* **114**, 241601, doi:10.1063/1.5095704 (2019).
- 7 Sloyan, K. *et al.* Discerning the Contribution of Morphology and Chemistry in Wettability Studies. *The Journal of Physical Chemistry A* **122**, 7768-7773, doi:10.1021/acs.jpca.8b04197 (2018).
- 8 Lu, J.-Y., Lai, C.-Y., Almansoori, I. & Chiesa, M. The evolution in graphitic surface wettability with first-principles quantum simulations: the counterintuitive role of water. *Physical Chemistry Chemical Physics* **20**, 22636-22644, doi:10.1039/C8CP03633K (2018).
- 9 Liu, J., Lai, C.-Y., Zhang, Y.-Y., Chiesa, M. & Pantelides, S. T. Water wettability of graphene: interplay between the interfacial water structure and the electronic structure. *RSC Advances* **8**, 16918-16926, doi:10.1039/C8RA03509A (2018).
- 10 Garlisi, C., Lai, C.-Y., George, L., Chiesa, M. & Palmisano, G. Relating Photoelectrochemistry and Wettability of Sputtered Cu- and N-Doped TiO₂ Thin Films via an Integrated Approach. *The Journal of Physical Chemistry C* **122**, 12369-12376, doi:10.1021/acs.jpcc.8b03650 (2018).
- 11 Chiesa, M. & Lai, C.-Y. Surface aging investigation by means of an AFM-based methodology and the evolution of conservative nanoscale interactions. *Physical Chemistry Chemical Physics* **20**, 19664-19671, doi:10.1039/C8CP03454K (2018).
- 12 Santos, S., Lai, C.-Y., Olukan, T. & Chiesa, M. Multifrequency AFM: from origins to convergence. *Nanoscale* **9**, 5038-5043, doi:10.1039/C7NR00993C (2017).
- 13 Santos, S. *et al.* The Mendeleev–Meyer force project. *Nanoscale* **8**, 17400-17406, doi:10.1039/C6NR06094C (2016).
- 14 Garlisi, C., Scandura, G., Palmisano, G., Chiesa, M. & Lai, C.-Y. Integrated Nano- and Macroscale Investigation of Photoinduced Hydrophilicity in TiO₂ Thin Films. *Langmuir : the ACS journal of surfaces and colloids* **32**, 11813-11818, doi:10.1021/acs.langmuir.6b03756 (2016).
- 15 Chia-Yun, L., Sergio, S. & Matteo, C. Reconstruction of height of sub-nanometer steps with bimodal atomic force microscopy. *Nanotechnology* **27**, 075701 (2016).
- 16 Lo Iacono, F. *et al.* General Parametrization of Persisting Long-Range Nanoscale Phenomena in Force Measurements Emerging under Ambient Conditions. *The*

- Journal of Physical Chemistry C* **119**, 13062-13067, doi:10.1021/acs.jpcc.5b02587 (2015).
- 17 Lai, C.-Y., Olukan, T., Santos, S., Al Ghaferi, A. & Chiesa, M. The power laws of nanoscale forces under ambient conditions. *Chem. Commun.* **51**, 17619-17622, doi:10.1039/C5CC05755H (2015).
- 18 Lai, C.-Y., Cozzolino, M., Diamanti, M. V., Al Hassan, S. & Chiesa, M. Underlying Mechanism of Time Dependent Surface Properties of Calcite (CaCO₃): A Baseline for Investigations of Reservoirs Wettability. *The Journal of Physical Chemistry C* **119**, 29038-29043, doi:10.1021/acs.jpcc.5b10595 (2015).
- 19 Chang, Y.-H. *et al.* Establishing Nanoscale Heterogeneity with Nanoscale Force Measurements. *The Journal of Physical Chemistry C* **119**, 18267-18277, doi:10.1021/acs.jpcc.5b04456 (2015).
- 20 Tzu-Chieh Tang, Carlo A. Amadei, Neil H. Thomson & Chiesa, M. Ion-Exchange and DNA Molecular Dip-Sticks: Studying the Nanoscale Surface Wetting of Muscovite Mica. *Journal of Physical Chemistry C* **Accepted** (2014).
- 21 Santos, S., Amadei, C. A., Tang, T. C., Barcons, V. & Chiesa, M. Deconstructing the governing dissipative phenomena in the nanoscale. *arXiv preprint arXiv:1401.6587* (2014).
- 22 Plummer, A., Tang, T.-C., Lai, C.-Y. & Chiesa, M. Nanoscale Hydrophilicity Studies of Gulf Parrotfish (*Scarus persicus*) Scales. *ACS Applied Materials & Interfaces* **6**, 16320-16326, doi:10.1021/am504568w (2014).
- 23 Amadei, C. A., Yang, R., Chiesa, M., Gleason, K. K. & Santos, S. Revealing amphiphilic nanodomains of anti-biofouling polymer coatings. *ACS applied materials & interfaces* **6**, 4705-4712 (2014).
- 24 Amadei, C. A., Lai, C.-Y., Heskes, D. & Chiesa, M. Time dependent wettability of graphite upon ambient exposure: The role of water adsorption. *The Journal of chemical physics* **141**, 084709, doi:doi:<http://dx.doi.org/10.1063/1.4893711> (2014).
- 25 Amadei, C. A., Tang, T. C., Chiesa, M. & Santos, S. The aging of a surface and the evolution of conservative and dissipative nanoscale interactions. *The Journal of chemical physics* **139**, 084708, doi:10.1063/1.4819267 (2013).
- 26 Amadei, C. A., Santos, S., Pehkonen, S. O., Verdaguer, A. & Chiesa, M. Minimal Invasiveness and Spectroscopy-Like Footprints for the Characterization of Heterogeneous Nanoscale Wetting in Ambient Conditions. *The Journal of Physical Chemistry C* **117**, 20819-20825, doi:10.1021/jp408984h (2013).
- 27 Katan, A. J., van Es, M. H. & Oosterkamp, T. H. Quantitative force versus distance measurements in amplitude modulation AFM: a novel force inversion technique. *Nanotechnology* **20**, 165703, doi:10.1088/0957-4484/20/16/165703 (2009).
- 28 Sader, J. E. & Jarvis, S. P. Accurate formulas for interaction force and energy in frequency modulation force spectroscopy. *Appl. Phys. Lett.* **84**, 1801-1803, doi:doi:<http://dx.doi.org/10.1063/1.1667267> (2004).
- 29 Garcia, R. & San Paulo, A. Amplitude curves and operating regimes in dynamic atomic force microscopy. *Ultramicroscopy* **82**, 79-83 (2000).
- 30 Garcia, R. & San Paulo, A. Attractive and repulsive tip-sample interaction regimes in tapping-mode atomic force microscopy. *Physical Review B* **60**, 4961 (1999).

-
- 31 Ramos, J. Tip radius preservation for high resolution imaging in amplitude modulation atomic force microscopy. *Appl. Phys. Lett.* **105**, 043111-043114 (2014).
- 32 Santos, S. *et al.* A method to provide rapid in situ determination of tip radius in dynamic atomic force microscopy. *Review of Scientific Instruments* **83**, 043707, doi:10.1063/1.4704376 (2012).
- 33 Maragliano, C., Glia, A., Stefancich, M. & Chiesa, M. Effective AFM cantilever tip size: methods for in-situ determination. *Meas. Sci. Technol.* **26**, 015002 (2014).
- 34 Font, J. *et al.* Spatial horizons in amplitude and frequency modulation atomic force microscopy. *Nanoscale* **4**, 2463-2469, doi:10.1039/C2NR12012G (2012).
- 35 Calò, A., Robles, O. V., Santos, S. & Verdaguer, A. Capillary and van der Waals interactions on CaF₂ crystals from amplitude modulation AFM force reconstruction profiles under ambient conditions. *Beilstein journal of nanotechnology* **6**, 809-819, doi:10.3762/bjnano.6.84 (2015).
- 36 Santos, S., Amadei, C. A., Verdaguer, A. & Chiesa, M. Size Dependent Transitions in Nanoscale Dissipation. *The Journal of Physical Chemistry C* **117**, 10615-10622, doi:10.1021/jp4039732 (2013).